Egert U (2006) Networks on Chips: Spatial and temporal activity dynamics of functional networks in brain slices and cardiac tissue. In: Urban G, (ed) BioMEMS, Springer Vlg., Dordrecht, NL, p. 309-350

PROOFS

Chapter 10

NETWORKS ON CHIPS

Spatial and temporal activity dynamics of functional networks in brain slices and cardiac tissue

Ulrich Egert

Neurobiology & Biophysics, Bernstein Center for Computational Neuroscience Freiburg, Institute for Biology III, University of Freiburg, Germany

Abstract: Cells of the same or different type in biological tissue closely interact and influence each other. Individual cells should therefore be studied in the context of the embedding cellular network. This particularly applies to the highly dynamic electrical activity of neuronal and myocardial networks, which continuously shapes the properties of these networks. Substrate-integrated microelectrode arrays allow the monitoring of network activity by extracellular recording *in vitro* with multiple electrodes simultaneously, thus providing access to the spatio-temporal patterns of electrical activity. This chapter gives an overview of approaches that allow investigations of the properties of neuronal networks in brain slices and cell cultures of cardiac myocytes. It presents and discusses examples for the application of these techniques in biomedical and pharmaceutical research.

Key words: microelectrode arrays, brain slices, neuronal networks, cardiac myocytes, analysis of local field potentials, drug screening,

1. INTRODUCTION

In many biological tissues the reciprocal interaction between individual cells and cell groups, together with the individual cellular properties, define the function of the network they form. These tissues and their interconnections are highly structured into networks over a wide range of spatial scales. Brain tissue, for example, is organized in functional pathways consisting of, e.g., layers and nuclei with specific cell type composition and local structure [1,2], glial networks and glia/neuron complexes around synapses on dendritic spines [3–5]. In cardiac tissue specialized transition structures form atrial and sinus nodes, conducting pathways, and working

muscle tissue [6–9]. The structural organization is essential for proper neuronal and cardiac network function, respectively. Pathological processes that affect this structure and the network composition of the tissue may, for instance, lead to epilepsy in neuronal tissue [10], to arrhythmia in cardiac tissue and to other disorders. These tissue architectures are initially brought about by developmental processes and are modified continuously by interactions of local network activity and cellular properties [11–15].

On a molecular level gene expression, the availability of receptors, and their phosphorylation and distribution may be changed by the activity in the network, directly or via its structure [16–18]. Arrays evaluating such changes, though not their fast dynamics are addressed in Chapter 5. Besides the obvious modulation of the overall action potential (AP) activity, excitation and inhibition in the network, the release of various neuromodulators, modulation of the extracellular K^+-concentration, etc., and the spatio-temporal distribution of activity are important, e.g., for short term synaptic plasticity and the balance of inhibition and excitation.

An increasing body of data collected in recent years indicates that the organization and activity of the local network continuously modifies the properties and the behaviour of individual cells on time scales as short as minutes or seconds. A network of excitatory and inhibitory neurons, for example, shapes each neuron, which, in turn, is an active part of this network. The properties of this neuron, its ion channel configuration, the distribution of synaptic strengths and locations, the fine structure of the dendritic tree, input impedance, etc., are continuously modified by the activity of the surrounding network [19–25]. The spatial and temporal structure of activity of the network as a whole ultimately represents information and its processing in the nervous system. Sequential single-cell studies are thus obviously limited in the suitability to correctly assess the properties and activity dynamics in a network, or even of individual cells in this network.

Similar influences of activity dynamics on cellular properties were observed in networks of cardiac myocytes [7, 29–31], with their specialized sino-atrial networks, activity dependent embryonic development, and complex interactions of multiple pacemakers under pathological conditions. Cardiomyocytes are interconnected through gap junctions, effectively forming a large syncytium. The electrical resistance of these pores can be modified and manipulated pharmacologically.

As a consequence the persistence or decay of a cellular response to a sensory or chemical stimulus will depend on the dynamics of the network activity. In addition the uptake and metabolization of a molecule by non-excitable cells in the vicinity will modify the effect of a drug. It is therefore necessary to evaluate the response of an individual cell to manipulations

affecting the network, e.g., by drug assays, electrical stimuli, and sensory stimuli in the context of the activity dynamics of that network. Whilst the optimal situation with respect to network integrity would be *in vivo* studies, these are often precluded when it is unacceptably difficult or time–consuming to implement multielectrode recordings, the desired control of the stimulus and environment, or to ensure access of the drug to the region of interest. In addition, the high complexity of the *in vivo* situation may hamper the interpretation of the results. Moreover, *in vitro* studies can be conducted with a higher throughput than *in vivo* experiments. Using *in vitro* preparations simplifies these experiments and allows better control of the cellular environment.

Quite early on the recognition of these relationships led to the request for and the development of microelectrode arrays (MEAs) for extracellular recordings from neuronal networks and cardiac myocytes [32–52]. These pioneer studies contributed valuable insights, but were hampered by the limitations of the computing technology available at the time. The advent of inexpensive computing power suitable for acquiring, storing and analysing the enormous data flow in such recordings renewed the interest in MEA techniques and spurred the development of suitable biological preparations, creating new perspectives for industrial applications. The use of MEAs to study local networks of excitable cells *in vitro*, in particular in brain slices and networks of cardiac myocytes will be the focus of this chapter.

Investigating the interaction within networks improves to our understanding of network function in general and of tissue architectures in particular. It helps our comprehension of the interplay between individual cells and network dynamics, and of the role of neuromodulatory transmitter systems within neuronal networks. From an application-oriented view, the including of small yet complex *in vitro* networks in, for example, a drug assay, should provide a more realistic picture of the overall effect of a tested substance. This, in turn, can be expected to enhance the predictability of a drug‘s effect on the intact organism and would help to identify the mechanisms by which this effect is mediated. Networks, for instance, readjust synaptic weights, adapting to modulations of ion channels or compensate changes otherwise. In addition, multielectrode recordings accelerate the collection of sample sizes necessary for statistical analyses[1]. The possibility to apply complex electrical stimuli through the MEA electrodes further expands the range of applications and bioassays, and

[1] For some applications optical recording using voltage–sensitive dyes [53–59] could be an alternative to this technique. The trade off between signal–to–noise ratio inherent to the technique, bleaching and the potential for phototoxicity, the lack of stimulation capability and the restricted recording time, however, limit their use.

contributes to the evaluation of pharmacological test substances in industrial research.

2. TECHNICAL ASPECTS AND UNDERLYING ASSUMPTIONS

Technically, MEAs can be categorized into active and passive arrays. The development of active arrays is guided by the idea that an array could be designed most compactly with integrated circuits, incorporating at the same time a supporting or growth substrate for the tissue and a recording device, including amplifiers, filters and a readout system. Whilst several successful components and prototypes have been developed, with their function demonstrated in recordings [33,50,60–63], for a long time the approach has been limited by the complexity of the technology required and the need for bio-compatibility. Currently these devices are still too expensive to produce for routine applications in the life sciences, and hence are not commercially available.

Passive arrays, on the other hand, in principle simply consist of insulated, thin-film metal electrodes (Fig. 10-1) or in some cases of doped and therefore conducting silicon. These electrodes are arranged on a carrier (Fig. 10-1), e.g., a glass slide, and are connected to separate, dedicated amplifiers, AD converters and data acquisition setup. Electrode arrays based on silicon bulk designs have also been developed as 3D needle arrays, similar to wire bundles, mainly intended for *in vivo* work, e.g., for long term recording, stimulation and as neuroprosthetic devices in the brain or peripheral nerves [64–66].

The first approaches towards substrate integrated electrode arrays used cultures of dissociated neuronal or cardiac tissue [34,36,37], following the idea that the general properties of a network can be restored from individual cells dissociated from native tissue and cultured to grow connective structures between them [27,67–76]. Application oriented studies evaluated such cultures for chemical sensors based on neuronal networks [77–79].

To investigate the electro-physiological properties of cellular interactions in intact tissue, on the other hand, preparations of, e.g., tissue cultures, cardiac papillary muscle, freshly prepared (‘acute’) brain slices, retinal tissue, etc., are well established. For acute slice preparations thin sections of the tissue are cut such that the propagation pathways and receiving cells are sufficiently intact to model the necessary functionality of the tissue [80,81]. Such slices are also maintained in tissue culture [82–88] (Fig. 10-8A) to allow some regeneration of damaged cells, removal of cell debris, and the re-balancing of excitatory and inhibitory synaptic weights.

Today MEAs suitable for routine electro-physiological recording to monitor the activity of neuronal populations *in vitro* are commercially available[2]. MEAs are used extracellularly to record low frequency local field potentials (LFP) and spike activity with substrate integrated electrodes at up to 70 sites in the tissue, i.e., the extracellular correlates of neuronal or cardiac APs. Such arrays are produced by thin-film photolithography with conducting leads of gold, indium–tin oxide or similar materials, and insulated with silicon dioxide, polyimide, or silicone polymers, which thus constitute the main contact surface for the cells. The actual electrodes are formed by an opening in the insulator 5–50 μm in diameter, exposing the tip of the leads underneath. During recording, a Helmholtz double layer builds up at the metal–electrolyte interface, effectively forming a high–pass filter [89–91]. The exposed electrode surface is usually coated with a porous material to lower the cut-off frequency of this high–pass filter by increasing the capacitance of the Helmholtz double-layer. This can be achieved, for instance, with iridium oxide, galvanically deposited platinum or sputtered titanium nitride (TiN) [87,92] forming a mechanically stable columnar structure (Fig. 10-1C). These modifications also increase the charge transfer capacity of the electrode, facilitating electrical stimulation via the MEA.

The recording conditions for MEAs are defined by several biophysical and biological factors (Fig. 10-2). The decisions about which specific MEA design to choose with respect to dimensions and materials, the data acquisition electronics and production techniques necessarily have to follow the biological question to be addressed. The design of an MEA used to record LFPs, for instance, should allow the coverage of an appropriate area of the tissue and should have electrodes with low impedance to reduce the lower cut-off frequency of the electrode. Such electrodes also allow the application of electrical current stimuli with low voltages, avoiding electrolysis. From a technical perspective, the metal–electrolyte interface and the type of contact to the cells define the interface between cell and electrode [91]. The stray capacitance across the insulator largely determines the frequency response, influences the signal–to–noise ratio of the recording, limiting the range of detectable biological signals, and therefore the questions that can be targeted in an experiment. To record LFPs (1–300 Hz) or other low frequency components, the electrode impedance and the lower cut-off frequency should be as low as possible. The MEAs used in our

[2] Links to developers of substrate-integrated arrays and corresponding equipment:
Multi Channel Systems, http://www.multichannelsystem.com;
AlphaMed, http://www.amedsci.com/english;
Ayanda Biosystems, http://www.ayanda-biosys.com;
BioCell-Interface, http://www.biocell-interface.com.

laboratories have 60 electrodes of 10–30 µm diameter on a 200 µm grid, with a coating of columnar TiN to minimize the impedance (Fig. 10-1).

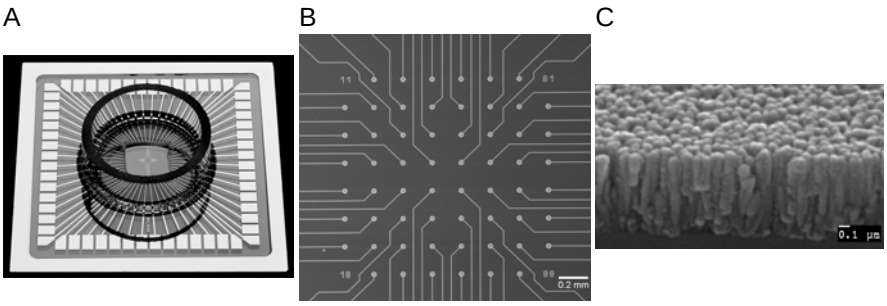

Figure 10-1. Design of a substrate integrated microelectrode array as used in our laboratory. (A) This version is on a 5×5 cm glass plate with conducting gold leads. A glass ring forms the recording chamber. (B) SEM micrograph of the recording area. The leads are insulated except for the center of the circles at the end of each lead. (C) SEM micrograph of a break-away of the electrode surface. Titanium nitride sputtered onto the electrode forms a columnar structure with a large inner surface, increasing the capacitance of the electrode area. MEAs from other producers are similar in their basic layout (Images by courtesy of Multi Channel Systems, Reutlingen and NMI Reutlingen, Germany).

2.1 System requirements

Analyses of spike-activity are now used for drug and toxin screening [77,93], research on pattern and rhythm generation in networks [94,95], and lately to control the movement of objects in virtual space based on the activity in neuronal networks [96]. Technically, recording single-unit spike activity[3] with a dominant signal frequency of about 1 kHz in cultures of dissociated neuronal cells allows smaller electrodes of relatively high impedance.

Besides ensuring tissue vitality (see below) and adequate conditions for cell culture[4], the probably most critical aspect for successful recording from acute slice preparations with MEAs is establishing and maintaining very close contact between tissue and electrode. From the perspective of the equivalent circuit, decreasing this distance increases the seal resistance between the electrode tip and the reference electrode (Fig. 10-2), and thus the signal–to–noise ratio in the recording. This can be implemented by either carefully pressing the tissue onto the array [98,99] or, probably less stressful for the tissue, gluing the slice onto the MEA using an adhesive coating, e.g., polyethylenimine (PEI) or cellulose nitrate, as used in our lab [100]. Both techniques mediate close and flat adhesion of the slice to the insulating surface of the MEA, allowing rapid superfusion of the tissue. After positioning the sliced tissue, the arrays are mounted into a setup holding the amplifiers, filters, and the data acquisition system.

Since acute slices have a high oxygen demand they rapidly decay without adequate superfusion. This needs to ensure rapid flow of buffer saturated with 95% O_2/5% CO_2 across the tissue, exchanging the bath volume 6–8 times per minute. Under these conditions, the O_2 partial pressure decreases rapidly with depth in the tissue (Fig. 10-3), but remains well above arterial O_2 pressure. Reducing the exchange rate results in suboptimal O_2 supply.

[3] In contrast to multi-unit and population activity the term single-unit activity is mostly used when the spikes in a train recorded extracellularly can be attributed to individual neurons. This may mean that (i) only spikes from one neuron were recorded, (ii) that the spikes from different neurons were separated using spike sorting, or (iii) that spikes from one neuron were separated from the rest. Multi-unit activity includes spikes detected with one electrode from several neurons that either were or cannot be separated, or in which individual spikes cannot be resolved at all. Population activity refers to contributions from large populations of neurons overlapping in time that consist of spikes and/or subthreshold membrane potentials.

[4] Culture conditions vary considerably for different cell types. An MEA specific technical improvement was published by Potter [97] using a gas permeable, but water vapor impermeable, membrane, which drastically reduces evaporation and the increase in osmolarity in the small culture chambers, a persistent problem even in high-tech incubators.

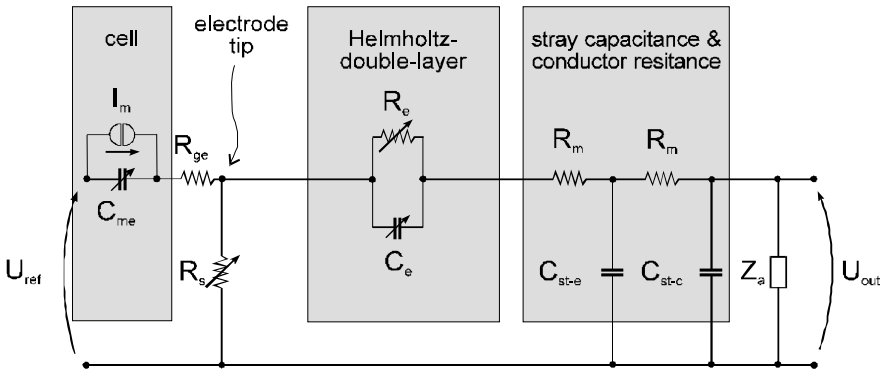

Figure 10-2. Equivalent circuit illustrating the main components of the recording configuration (modified from [101]). For extracellular recording the cell is considered a current source producing a voltage drop across the voltage divider formed by the resistance R_{ge} through the buffer between cell membrane and electrode tip, the seal resistance R_S between electrode tip and reference electrode and the impedance of the Helmholtz double-layer (R_e, C_e) in series with the resistances of the conducting leads Rm. The impedance of the Helmholtz double-layer at the metal–electrolyte interface and the stray capacitances across the insulator in the electrolyte solution (C_{st-e}) and cables (C_{st-c}) create a bandpass filter. Increasing the electrode surface increases C_e and thus reduces the electrode impedance, improving its recording properties.

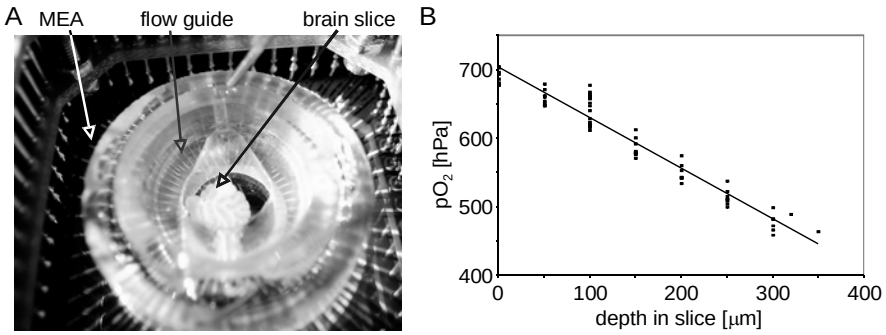

Figure 10-3. (A) Superfusion arrangement for MEA recording. A glass ring forms the recording chamber. The flow guide inserted into this ring reduces the volume to 0.5 ml and ensures a smooth flow of buffer across the tissue. (B) Oxygen partial pressure at increasing depth within the slice. O_2 was measured with a fibre optic system (PreSens Precision Sensing, Regensburg, Germany) with a 30 μm sensor. When superfused with buffer saturated with 95% O_2/5% CO_2 at 6–8 exchanges/minute, the O_2 supply is well above arterial O_2 partial pressure (approx. 120 hPa) at any depth in the tissue at room temperature. The slope of the O_2 partial pressure depends on temperature and superfusion rate.

3. ORIGIN OF THE SIGNAL RECORDED

As described by Rall [102,103], the time course of the potential recorded extracellularly is related to the time course of the first derivative of the membrane potential of the cell studied. This corresponds to the time course of the depolarizing and hyperpolarizing currents across the membrane. Na^+, K^+, and Cl^- flowing through ion channels in the membrane and compensating capacitive currents flowing simultaneously in the opposite directions carry the major part of these currents. The spatial distribution of the latter very much depends on the distribution of the internal and leak resistances of the cell, which in turn are influenced by its morphology. As a result of the complex and ramified neuronal dendritic tree, it is essentially impossible to fully reconstruct the transmembrane potential from an extracellular recording [104], neither in its amplitude nor its time course. This also indicates that the extracellular signal from thin axons will be minor, as only weak currents flow across their small membrane area during an AP. In addition, at any one site in the extracellular space the local potential will be the sum of contributions from all these current sources within the recording horizon of the electrode [100,105]. In native tissue this encompasses a large number of cells.

The situation is somewhat simplified if the cell or tissue under study can be considered large with respect to the electrode, homogeneous in its morphology and if the seal resistance is high. This is achieved when cardiac myocytes are cultured on MEAs. These cells form extensive layers of cells coupled through gap junctions. Under suitable culture conditions they develop spontaneous rhythmic contractions with large APs propagating across the array (Fig. 10-4). This configuration allows intracellular recordings simultaneously with extracellular MEA recordings [105]. Analysis of the intra- and extracellular time course indicates that the current components mentioned above can in part be identified in the MEA recording. In the regions initiating the activity a sharp negative peak in the MEA recording accompanies the depolarizing upstroke of the intracellular AP that is mainly driven by Na^+. Conversely, a positive peak parallels the repolarization phase carried by K^+. At recording sites along the propagation pathway a positive peak, reflecting passive outward currents, preceded the negative peak.

These experiments thus confirm the prediction that AP properties can be estimated from FPs and enable analyses of the cardiac AP duration based on MEA recordings.

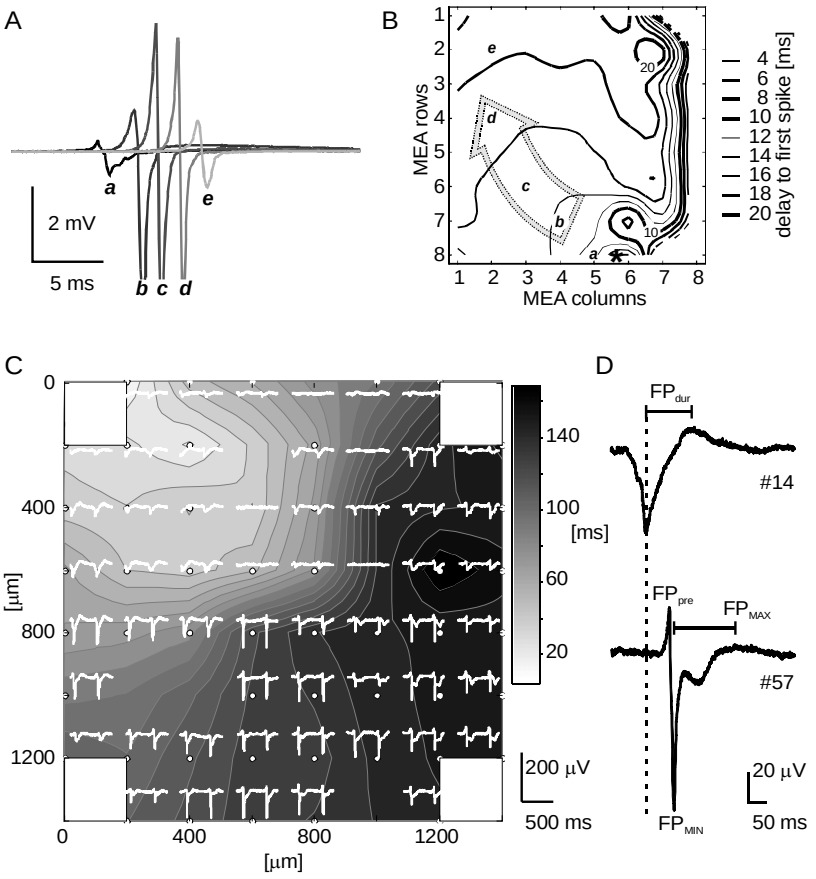

Figure 10-4. Spread of excitation in a cell culture of neonatal cardiac myocytes after 6 days in culture. Based on recordings from 60 electrodes in this confluent cell layer, we reconstructed the spread of excitation through the tissue. (A) The delays and changes of the spike shape were readily visible in these sample traces recorded at 5 positions along the path of propagation (a–e in B). (B) In this case the origin of excitation lay in the bottom right corner of the MEA (approx. at the asterisk). Excitation spread towards the top left corner, as indicated by the arrow. The isochrones (interpolated based on 60 recording positions) give the delay of the spike minimum at each position with respect to the earliest peak. Only a thin layer of cells that did not visibly contract covered the right side of the array (columns 7 & 8). The negative peaks in A were clipped graphically. (C) Overlay of the FP recording and false color rendering of the delays of the first negative peak on each electrode to the earliest occurrence on the MEA [105]. (D) Identification of the FP minimum (FP_{MIN}) marking the onset of the AP and the maximum (FP_{MAX}) indicating the downslope of the AP.

4. SPATIAL RESOLUTION

Because of the extensive and overlapping dendritic trees of many types of neurons, it is not straightforward to identify where the neuronal signal recorded at an electrode was generated. Obviously the amplitude of neuronal spikes will decrease with distance. A second scaling factor is the size of a neuron, or rather its membrane, as can be deduced from the relation of the extracellular signal to the currents flowing across the membrane. Since the specific membrane resistance is constant (unless ion channels open), small neurons have a lower capacitance and a higher input resistance. The charge required to maximally depolarize their membrane is thus smaller than for large neurons. Their extracellular signal is therefore smaller than that of larger cells. This ambiguity impairs the identification of the spatial location of the signal source in single unit recordings. We investigated this question in MEA recordings from acute parasagittal slices from the rat cerebellum (Fig. 10-5). The structure of the cerebellum is such that in these slices the large, essentially two-dimensional, dendritic tree of the Purkinje cells lies flat on the MEA, extending into the molecular layer only. Their cell bodies are aligned in the Purkinje cell layer. These cells are spontaneously active at high rates. To determine the recording horizon of MEA electrodes we probed the region around one MEA electrode that picked up spikes with a single, separate micropipette electrode. We then measured the amplitude distribution of the potential recorded with the micropipette when a spike was detected on the MEA electrode as a function of the distance between the two electrodes (Fig. 10-6). The resulting potential surface indicated that the recording horizon of such an electrode has a radius of approx. 60 µm [100]. The fields of view of the MEA electrodes spaced on a 200 µm grid therefore did not overlap. This footprint is obviously valid for unit spikes only, and the electrode horizon scales with the size of the cell for reasons explained above. Extensive dendritic trees in some cases will allow the recording of spikes at greater distances. The lack of conspicuous correlation between spikes recorded at neighbouring electrodes further supports that there was no detectable overlap between the recordings at neighbouring electrodes (Fig. 10-6D) [100].

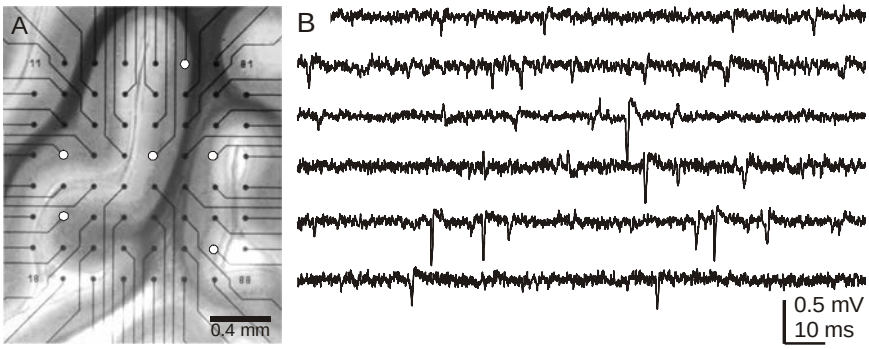

Figure 10-5. (A) Cerebellar slice from a juvenile rat in the recording situation. The layers of the cerebellar cortex and the white matter are clearly distinguishable (dark: myelinated fibers in the white matter; next layers: granule cell layer, Purkinje cell layer (only one cell body in thickness) and molecular layer with the dendritic tree of the Purkinje and Golgi cells). Fissures separate the lobes of the cerebellum. (B) Raw signal recorded at the electrodes marked in A. Spikes can be readily detected. The signal–to–noise ratio is typical for this preparation, and typically even higher in organotypic cultures of such slices.

5. LFP AND PLASTICITY

The discussion in the previous section has already indicated that, given the number of neurons and their neurites located within the recording horizon, FPs created by these neurons overlap in time and add up linearly. Because of this summation, contributions by single neurons occurring more or less synchronously may therefore become indiscernible. On the other hand, because of this spatial integration signals from synchronized events, which would normally be too small to be identified, may rise above the noise level and become detectable. This is particularly interesting for excitatory and inhibitory postsynaptic potentials (EPSPs and IPSPs). These events, depolarising the membrane by less than 10 mV and lasting several tens of milliseconds, overlap in time in this situation and become visible as population PSPs (pPSPs) extracellularly. Mixed with population spikes they constitute LFPs. The long time constants of the individual EPSPs and IPSPs and their temporal distribution in the population lead to dominating frequencies below approx. 300 Hz in the LFP. These signal components can be separated from spike activity consisting mainly of components above 500 Hz by filtering. The detailed frequency composition of LFPs is quite variable, ranging from low-frequency response components, with time constants up to hundreds of milliseconds, to approximately 300 Hz. Spikes may contain components up to about 3.5 kHz.

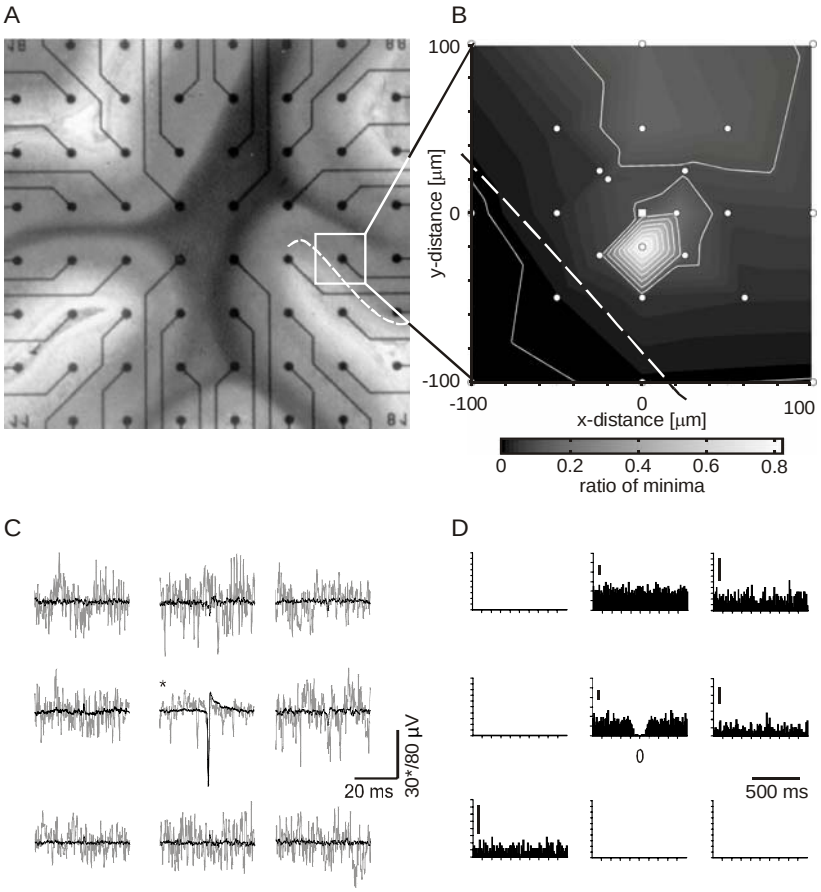

Figure 10-6. Spike activity is the basic single-neuron activity recorded with extracellular electrodes. In the cerebellum, for example, Purkinje cells are firing spontaneously. (A) The micrograph illustrates the structure and dimensions of an acute parasagittal slice of a rat cerebellum on an MEA. (B) Relative strength of the peak recorded with a micropipette at the positions marked with white dots. From the voltage measured with the micropipette when a spike was detected at the reference MEA electrode (square), we calculated the ratio of this voltage and the voltage at the MEA electrode. The greyscale image shows the interpolated distribution of these values, indicating that the background level is reached at approx. 60 µm from the maximum. The bright region approx. 20 µm below the MEA electrode identifies the likely position of the cell body. The dashed lines in A and B indicate the Purkinje cell layer. (C) Single (grey) and spike-triggered average (black) recordings at nine neighbouring MEA electrodes, centered on the spike time of a neuron at the central electrode. There were no detectable spikes at the surrounding electrodes that could correspond to the spike at the centre electrode. Even the average traces show at best only small peaks that are not detectable at this noise level. (D) These small peaks were not sufficient to result in peaks in the cross correlograms [100].

Common fields of research are, for example, the investigation of synaptic plasticity, epileptogenesis, the role and origin of specific frequency bands such as the > 30 Hz gamma band, the 4–10 Hz theta rhythm found in the cerebellum and brain stem, and the acetylcholine modulated beta rhythm (10–30 Hz) [106].

With slice preparations it is possible to address several of these topics. A classical preparation for investigations on long-term potentiation (LTP) is the hippocampal slice, a region involved in memory formation and spatial orientation. It can be cut so that there are three major populations of synapses and local connections of, e.g., inhibitory interneurons (Fig. 10-7A). The strength of these synapses depends on the history of the incoming activity and the efficacy with which the activation of the synapses contributed to the firing of the postsynaptic cells. The pyramidal cells in the CA3 subregion of the hippocampus, for example, project onto the dendrites of the pyramidal cells in the CA1 region along the Schaffer collateral pathway. The efficacy of the synapses formed by these axons can be enhanced by high frequency stimulation delivered through either MEA or separate wire electrodes. The distribution and dynamics of the responses to such stimuli, as well as of the synaptic plasticity determined from changes of the response magnitude (Fig. 10-7B) can be determined from LFP responses in MEA recordings.

With the interpretation of the origin of negative and positive voltages given above, one can, with due caution, now describe some of the dynamics of the voltage pattern as a sequence of the propagation of axonal spikes, postsynaptic activation in the dendritic layers of the CA region, and post-synaptic population spike activity. Pre- and postsynaptic elements of the waveform can be identified by subtracting the response obtained after blocking synaptic transmission, e.g., by removal of Ca^{2+} from the saline, from the response obtained in normal recording buffer. The outstanding mechanical stability of the recording configuration makes these analyses highly reproducible and easy to do. To determine the location of the synaptic currents, current source density (CSD) analysis can be a suitable tool if the tissue has a laminar structure and the electrode spacing is sufficiently small to distinguish all layers [107–113]. CSD analysis was originally used to analyse LFP responses sampled sequentially at regular intervals along the track of an electrode pushed into the brain. It relies on the assumption that the general structure of the tissue changes along one dimension only, e.g., as in layered tissues like the neocortex or the lateral geniculate nucleus. Novak and Wheeler extended this analysis to two dimensions in MEA recordings of the hippocampus [108,109]. They approximated the procedure by applying a two-dimensional Laplacian kernel to the voltage map gained from MEA recordings. As any procedure working on sampled data, this assumes that the

spatial frequencies of the current maps are sampled at sufficiently narrow spatial intervals. Most MEAs used, however, do not meet this requirement. Filtering for low spatial frequencies alleviates this problem, but restricts the interpretation to relatively large current sinks and sources [106].

6. NETWORK DYNAMICS AND EPILEPTIFORM ACTIVITY

For long-term studies brain slices can be maintained in tissue cultures on MEAs, enabling experiments that require either intermittent or continuous recording and stimulation of the tissue [87,114]. Tissue cultures on MEAs were used to investigate neuronal regeneration [114], neuronal development [98,99,115,116], rhythmogenesis [75,76,117], circadian rhythms [118], and the initiation of epileptiform activity [88,108,109]. Cultures of hippocampal slices maintain their general anatomy with the principal areas, layers and connections outlined above (Fig. 10-8A). In these cultures spontaneous spike activity develops even though the input pathways are severed. A network of inhibitory interneurons contributes to the stability of the electrical activity. Interrupting this inhibitory transmission by blocking $GABA_A$ receptors unbalances the network and leads to synchronous, epileptiform activity (Fig. 10-8). With respect to the treatment of epilepsy, this transition from desynchronized balanced spike activity to highly synchronized propagating population activity is particularly interesting because it marks the onset phase of the epileptiform activity dynamics. This transition could potentially be more easily treated than fully developed epileptic seizures.

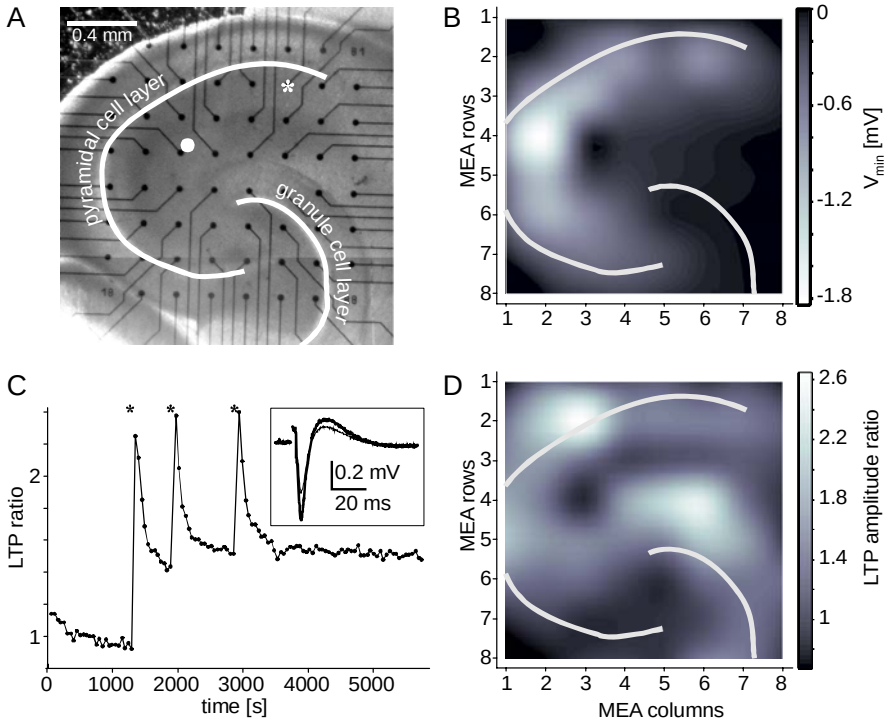

Figure 10-7. Analysis of long-term potentiation (LTP) in an acute slice of the hippocampus. The distribution of LFP properties and changes in hippocampal slices (A) can be assessed with MEAs. (B) Population spike amplitudes induced by electrical stimulation (at the white dot in A) can reach more than 2 $mV_{peak\ to\ peak}$, with pronounced minima (V_{min}) in the pyramidal cell layer and the proximal apical dendrites. (C) Brief bursts of stimuli (*, three repetitions) induced LTP, drastically increasing the response amplitude. The insert shows a typical response profile (thin line: before LTP induction, thick line: recorded at 3100 s) after high frequency stimulation. The responses recorded at the asterisk in A increased temporarily by up to 140% (post-tetanic potentiation) and persistently by more than 50%. (D) The distribution of the increase of the response amplitude is visualized as an interpolated pseudo-colour image. Significant increases of the response are mainly found in areas activated by orthodromic or antidromic activation of synapses in the CA region and the dentate gyrus [119].

The preparation thus provides a model in which the synchronization of activity in time and space can be monitored and related to the structure of the network. This requires mapping of the LFP data onto the dynamics of activity in the network, i.e., the spatial and temporal distribution of synaptic and spike activity. Extracting these distributions from the LFP by separating the average contribution of a neuron and the temporal distribution of firing

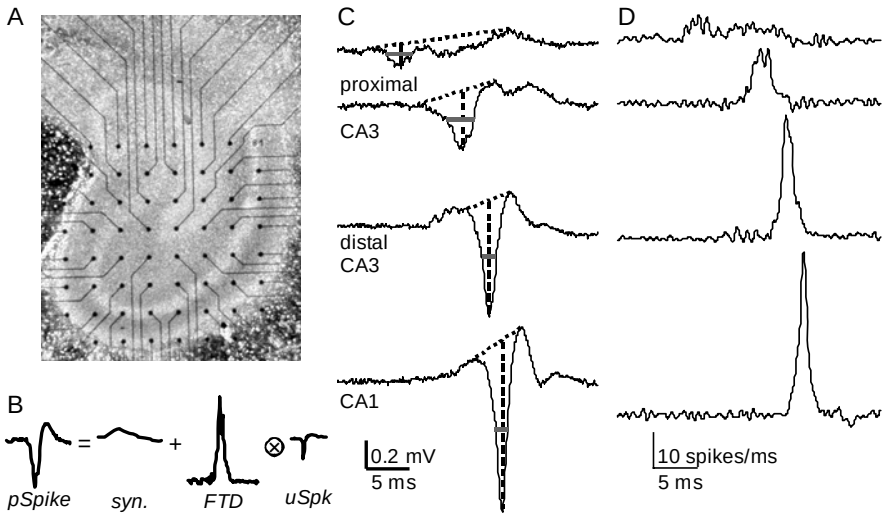

Figure 10-8. Population spikes and firing time distributions. (A) Organotypic culture of a hippocampal slice on an MEA. Inter-electrode distance is 200 µm. (B) Population spikes (pSpike) detected in LFPs can be seen as a convolution of the firing time distribution (FTD) of the local neuron population with a unit spike (uSpk) plus contributions of synaptic events (syn). Based on this model, the FTD can be estimated by deconvolving the LFPs (C) with the average single-unit spike used as uSpk. The synaptic event residual is then estimated from negative values of the firing time distribution. After subtraction of this residual the deconvolution is repeated resulting in the FTDs in (D). In this recording of an epileptiform spike the population activity synchronized as it propagated from the initiation site in CA3 towards CA1, resulting in sharper FTDs with higher peak spike rates (see also Fig. 10-9) (modified from [88]).

times can create this link. The contribution of a cell within the recording horizon of an electrode can be estimated by averaging the waveforms of all spikes detected at an electrode. Behind this approach stands the assumption that the composition of the neuronal population contributing these spikes reflects the population participating in generating the LFP. The population spike can then be considered as the convolution of the average neuronal spike and the distribution of the times at which the cells within the recorded volume fire (firing time distribution, FTD) (Fig. 10-8). The structure of the FTDs at the MEA electrodes was compared to the dynamics in computational network models built with hippocampus-like neurons and architecture. The simulated activity quite faithfully reproduced the dynamics observed in the culture, indicating that only a few cellular parameters need to be changed to induce the transition (Fig. 10-9) from normal to epileptiform activity. Such computational models could be used to identify the mechanisms and factors influencing the spatio-temporal dynamics of the FTD during the transition from irregular activity to synchronized firing. This

could lead to new targets for the development of anti-epileptic drugs [88,121].

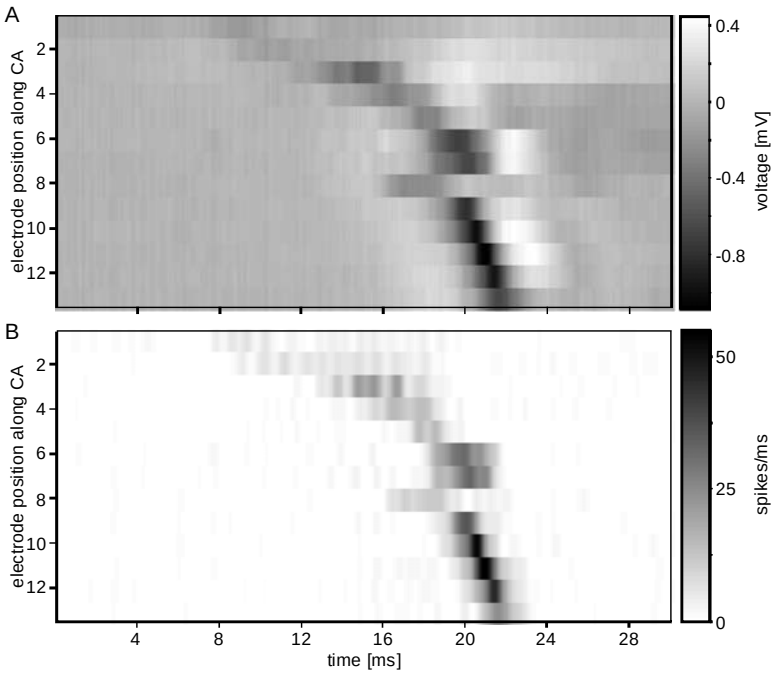

Figure 10-9. LFPs and corresponding FTDs as pseudocolour representation. (A) Grey-scale rendering of the LFPs voltage recorded at successive electrodes along the pyramidal cell layer in an organotypic culture of the rat hippocampus on an MEA. The LFPs were epileptiform spikes provoked by disinhibiting the network with the $GABA_A$ receptor blocker bicuculline. As the population spike propagates along the pyramidal cell layer from CA3 (top) to CA1 (bottom), its amplitude increases and its temporal width decreases. (B) FTDs were calculated from the LFPs as described above. They now represent the time course of spike activity in the underlying network. The dynamics of this activity and the conditions for the initiation and propagation of this type of epileptiform activity was further analyzed in the simulations of networks with hippocampus-like properties. The network reproduced most of the phenomena observed in MEA recordings [88, 120].

7. DRUG TESTING WITH MEAS

One of the incentives for developing the MEA technique and the necessary biological preparations was that they might be useful tools for drug evaluation in pharmaceutical industry. Several aspects contributed to

this expectation: one concept is that the insights gained from network studies will facilitate the search for new pharmaceutical drugs and the evaluation of their potential benefits and risks in the pre-clinical screening phase. In addition to the approach to evaluate network function to improve the predictive value of *in vitro* experiments, MEA studies through parallel recording could decrease the time needed to collect statistically relevant sample sizes, increase the throughput of test substances and reduce the associated costs per data point. Because of the mechanical design parallel, semi-automatic recordings from multiple setups become feasible. MEAs allow multiple sterile measurements from the same preparation where needed, e.g., in regeneration studies, and they can be used to simultaneously assess the response distribution in a population, given that the responses are generated independently.

7.1 Using Network Properties as Endpoints in Drug Assays

Some properties of electrical activity in the nervous system are a direct consequence of neuronal interactions that cannot be detected in single cell studies. Amongst these are spatially distributed oscillations of spike activity, observable, for example, in correlation analyses. These patterns have gained renewed interest since it was discovered that *in vivo* the γ-frequency band (30–70 Hz) is associated with the detection of contiguous objects in visual stimuli [122]. The mechanisms mediating and controlling these and other network patterns are, however, not always clear. β-wave (10–30 Hz) rhythms are known to be modulated by connections using acetylcholine as a transmitter [106]. This type of activity was found in acute slices of the hippocampus and was successfully mapped with MEA recordings [106]. The dynamics and spatio-temporal extent of these oscillations as well as mechanisms controlling them can be rapidly investigated *in vitro* using MEAs. Carbachol, a cholinergic agonist, induced such oscillations, which may serve as indicators of cholinergic action of a test substance (Fig. 10-10).

7.2 Assessing Distributions of Neuronal Responses to Dopamine

Dopamine is an important neuromodulating transmitter known to be involved in a wide spectrum of physiological and pathological processes. The receptors are classified into various subtypes, which can be linked to the different functions of dopamine. D_1 receptors are, for example, linked to learning and reward, D_2 receptors to Parkinson‘s disease, and D_3 receptors to schizophrenia. Identifying sites of action and responses to the presence of an

agonist at these receptors in the network is therefore an important topic in industrial drug screening. Most neurons, however, express several receptor subtypes in combination, hampering the analysis of a particular substance's selectivity and specificity. Only a few areas in the brain have separable populations of neurons with D_2 and D_3 receptors, interspersed with neurons lacking them. An electro physiological study therefore faces a heterogeneous response profile of the population and needs to record from a large number of cells to collect a representative sample. In the vermis, the central ridge of the rat cerebellum, it was discovered that lobes 9 and 10, the hindmost ventral lobes, have a high density of D_3 receptors but lack D_2 receptors [123].

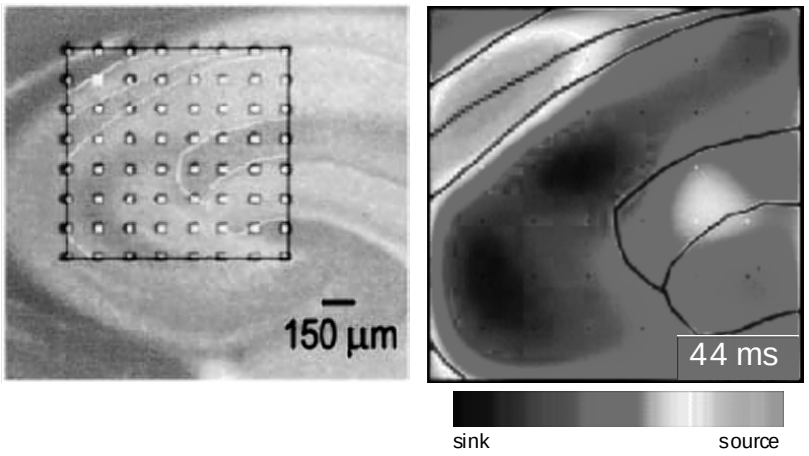

Figure 10-10. Current source density analysis of carbachol induced β-wave activity in a rat hippocampus slice. (A) This high-density array covers parts of CA3 and CA1 in the slice. (B) On this snapshot taken during β-wave activity the sources are located in the pyramidal cell layer, sinks in the dendritic tree, indicating excitatory synaptic activity. Though induced by carbachol, the activity depends on glutamatergic transmission, probably involving several local networks, including inhibitory neurons. The pattern propagated with a 23 Hz cycle (modified from [106]).

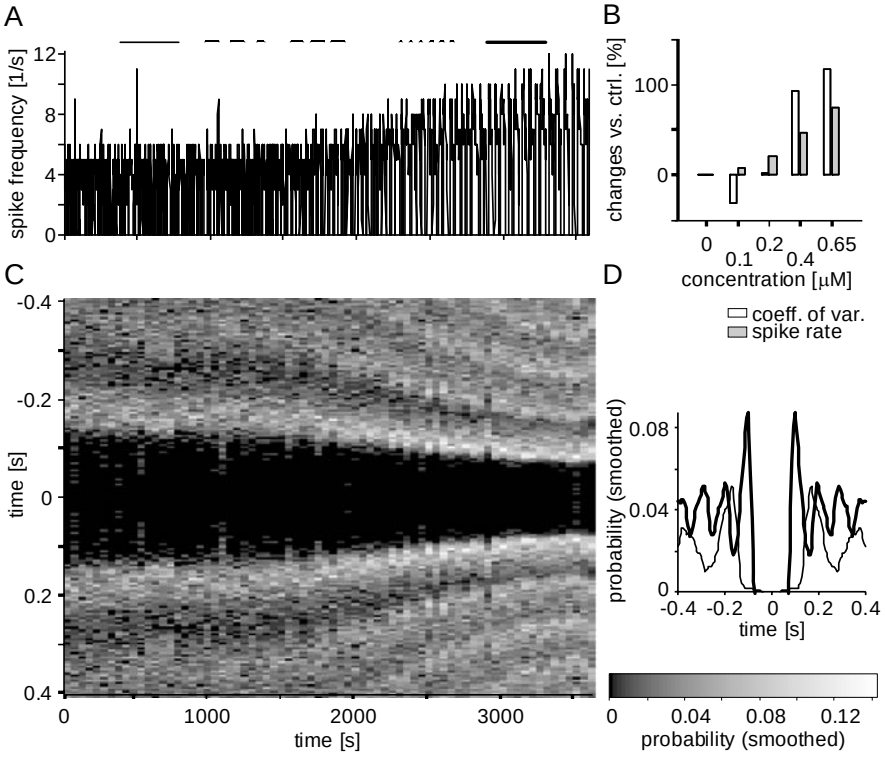

Figure 10-11. Using spontaneous spike activity for dopamine assays. (A) Firing rate of spontaneous activity in a cerebellar slice. Activity fluctuates in a burst pattern. Intra-burst activity increases when the dopamine D_2/D_3 receptor agonist quinpirole is applied in increasing concentrations. Dashed lines indicate the evaluated time window and the application of different concentrations of the drug. (B) The overall activity is summarized in the mean rate and the Fano factor as a measure of the local variability of the spike count for each concentration. (C) The dynamics of the autocorrelation during the burst illustrates a pattern of regular firing. The mean firing frequency within the burst increased with the drug concentration. (D) Autocorrelograms for two intervals resp. drug concentrations [124, 125].

Other lobes in the cerebellum in turn do express the D_2 but not the D_3 receptor. We therefore investigate the modulation by dopaminergic drugs of spontaneous spike activity in acute slice preparations from the cerebellum of neonatal rats.

Since, as described above, spike activity detected in MEA recordings from the cerebellum reflects electrically and physiologically independent spike sources, each experiment provides a sample from a population of cells. We therefore analyse the modulation by dopaminergic drugs of spontaneous spike activity in acute slice preparations from the cerebellum of neonatal rats. The geometry of the MEAs used in our laboratory allows the experimenter to record from cells in up to three lobes simultaneously, with

several electrodes in each of them. This approach thus provides a sample of the populations with different receptor sets. Spikes are readily detected in these preparations (Fig. 10-5). Fig. 10-11 illustrates the changes of the spontaneous activity found at an electrode in one such experiment. The temporal structure of the spike activity has a burst component with regular intra-burst intervals between spikes and intermittent pauses of up to several seconds. The autocorrelation, reflecting the periodicity of the spike activity, reveals this structure with distinct side bands. The dynamics of the changes induced by a drug at increasing concentrations is suitably captured by a pseudocolour representation of the autocorrelation calculated for spikes within a moving time window and summarized in correlograms of the relevant phases of the experiment. From such experiments we determined the typical response profile of the neuron population in a cerebellar lobe to drugs with known receptor selectivity. These 'finger prints' summarize the distributions of the directions of change of the above parameters (Fig. 10-12). We expect that this technique will allow the rapid identification of the response profile for a given drug by comparison with the respective fingerprints of known substances.

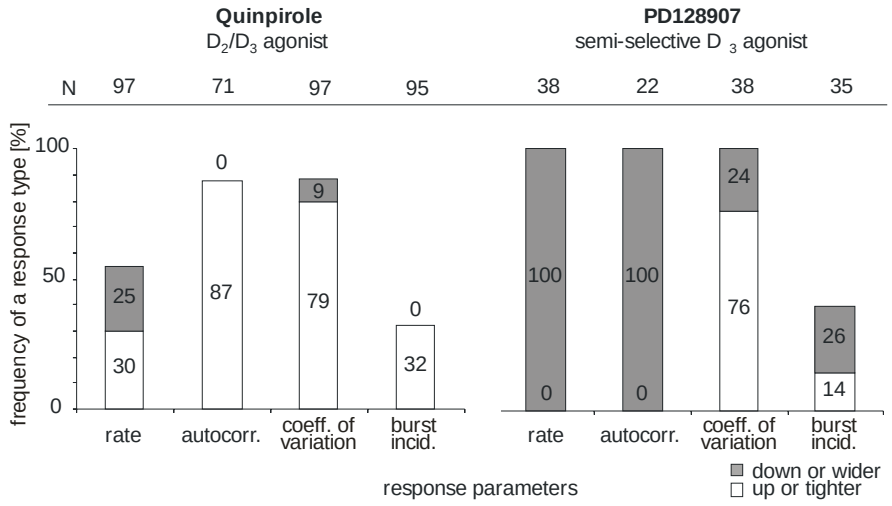

Figure 10-12. The distribution of the responses, which are highly variable across the population recorded, forms a fingerprint-like pattern that is different for each of the drugs tested. These patterns could help to identify related response types [124,125].

7.3 Cardiopharmacology

In cardiology the spread of activity, its embryonic development and its pathological conditions, such as arrhythmias, are highly important issues (Fig. 10-4). Here the continuously contracting tissue poses quite a challenge for recordings with conventional microelectrodes. A comparatively slow pacemaker current depolarizes the cell to a threshold at which a fast AP is elicited. The AP is dominated by an inward Na^+-current and repolarized by outward K^+-currents through various ion channels. The characteristic plateau phase of the cardiac AP is sustained by a Ca^{2+} inward current whose time course varies across cells at different positions within the cardiac tissue, i.e., their functional differentiation. The relative strengths of these currents are highly critical to ensuring the correct succession of excitation and propagation in the cardiac muscle and thus its physiological function and performance. The electro physiological measurement and analysis of these currents, reflected in the time course of the membrane potential, is therefore an important field in basic research and routine analysis in pharmacological research and development.

The AP duration and its variability is a critical parameter in safety pharmacology. *In vivo* this property of the AP is reflected in the interval between the Q and the T wave of the electro cardiogram (duration of the QT period). Under certain conditions prolongation of QT duration has been linked to lethal side effects of drugs [126–128]. Test for QT prolongation have therefore become a mandatory requirement in safety pharmacology [127]. This necessitates tests on a large number of drugs, either under development or already on the market. Using *in vivo* tests is inconvenient because of the associated high costs and low throughput. Since several ion channels and receptors are involved in the dynamics determining the AP duration, with the HERG channel being the most important one, data obtained from cell lines expressing a single ion channel type can be misleading, resulting in false negatives or false positives. The interplay of the various cellular mechanisms is better captured in native cells.

In recordings with conventional electrodes, motion of the tissue with respect to the electrode may not only damage the cells but also produces motion artefacts in the electrical signal that prevent a detailed analysis of the FP. It is therefore generally very difficult, and often impossible, to determine spatial dynamics of excitation, details of the waveform and long term changes, let alone perform multiple simultaneous measurements in cardiac tissue. The combination of MEA recording with cultures of cardiac myocytes thus marks significant progress, supported by the fortuitous situation that the contraction is essentially isometric at the tissue surface adhering to the substrate. The signal amplitude can be very high and motion

artifacts are not observed. Substrate-integrated electrodes thus create a unique mechanical configuration forming a highly stable recording situation. This allows the observation and analysis of activity in contracting cardiac tissue over periods of several days, enabling a new type of experiments on cardiac development [129,130]. Numerous studies have exploited this advantage to study signal to electrode coupling, arrhythmia or signal propagation in cardiac myocyte cultures.

Substrate integrated MEAs also allow the assessment of the duration of the cardiac AP. As shown above, changes of the AP duration can be estimated in cell cultures by analysing the waveform of the FP recorded with MEAs (Fig. 10-4). Considering the FP as a function of the inverse of the first derivative of the membrane voltage with respect to time, the strong depolarising Na^+ current and the depolarising K^+ current can be identified as leading negative and trailing positive peaks in the FP. The interval between these peaks is defined as FP_{dur} and is proportional to the QT interval [105]. MEAs thus provide a simple tool for implementing semi-automatic assays on such cultures. Recent experiments validated the approach using drugs with well-known effects on the QT duration (Fig. 10-14). The concentration-dependent response profiles found in cardiomyocyte cultures on MEAs were very similar to those found *in vivo* [126, 131, 132]. These results led to the development of simplified, and therefore inexpensive, single usage recording arrays on printed circuit boards. The electrodes with 100 µm diameter can be integrated in the 96-well plate format commonly used with pipetting robots for routine applications. Such arrays are currently tested for medium throughput QT screening in industrial drug safety pharmacology (Fig. 10-13).

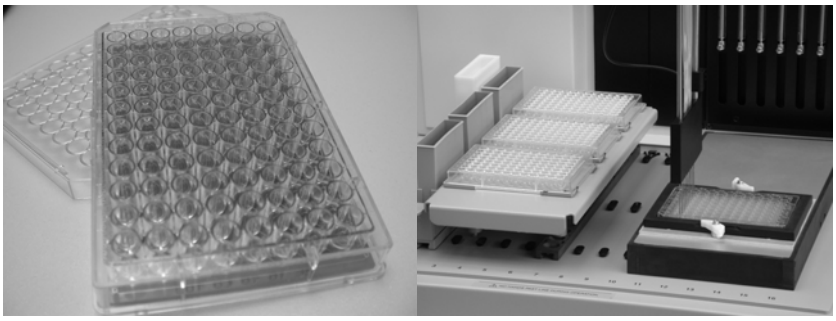

Figure 10-13. Prototype of a system with substrate-integrated microelectrodes produced on printed circuit boards with standard 96-well plate format. In this case cardiac myocytes will be cultured on the arrays for tests of QT prolongation. The standard 96-well layout and robot compatibility facilitate the adaptation to common laboratory procedures and increases the

throughput of the assay. The data acquisition electronics is integrated onto the base plate (images by courtesy of Multi Channel Systems, Reutlingen, Germany).

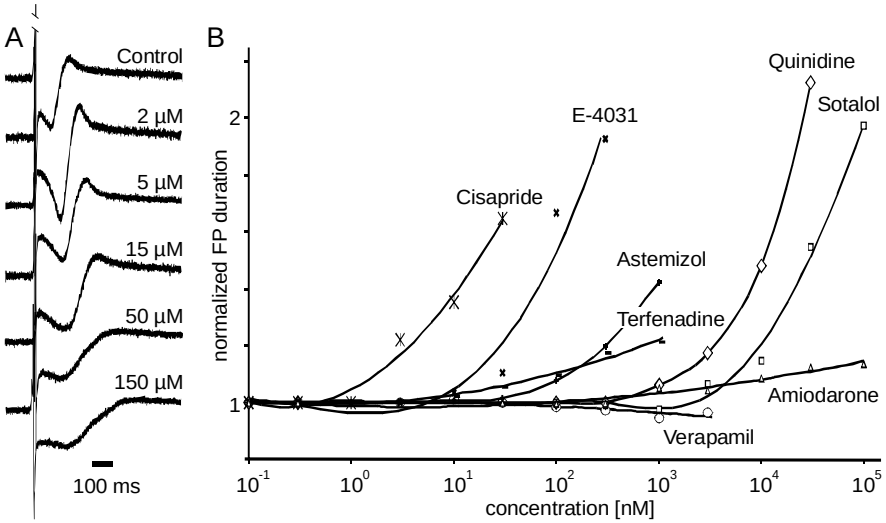

Figure 10-14. MEA recordings allow *in vitro* prescreening for QT prolongation in cardiac myocytes. (A) Individual field potentials (FP) recorded in a chicken cardiomyocyte culture on an MEA during treatment with the sodium channel blocker quinidine, which increases the duration of the cardiac AP and of the QT interval in the *in vivo* electrocardiogram. The *in vitro* FP waveform shows conspicuous peaks correlating with onset and end of the AP (see Fig. 10-4). The AP prolongation elicited by this drug is clearly visible in the FP. (B) All drugs tested thus far changed the FP duration as expected from ECG recordings [126,131].

8. DATA ANALYSIS

A critical aspect in all multielectrode recording is the processing of the large amount of data acquired in each experiment. For a 60-electrode array, for example, continuous recording at a sampling rate of 25 kHz with a 12 bit AD converter amounts to approximately 3.2 MB per second. Today it is simple to continuously store this and higher data rates to hard disc, nonetheless pre-processing, visualizing, analysing, and searching these data for suitable descriptive parameters becomes time consuming, in particular when interactions between neurons are of interest. It exceeds the scope of this chapter to discuss such data analysis in detail. We shall, however, give a short outline of the demands appearing in MEA experiments and provide links to literature and software available for this purpose.

The analysis process can be segregated into online and offline analyses. Online analyses are needed to monitor the experiment and for quick analysis of important parameters, such as spike rate, peri-stimulus time histograms (PSTH), extraction of minima and maxima of a waveform and their timing, etc. Offline analyses may either require more processing time or more of the experimenter‘s attention than is available during an experiment. Other analyses may require pre-processing, e.g., to remove artefacts, sort spikes recorded from different neurons at the same electrode by more sophisticated methods, detrending, and the like. In particular, analyses of correlations or inter–dependencies of activity across recording sites and time is generally not possible online. Some visualizations might be feasible but are not useful in real time, e.g., animated displays of the spatial dynamics of voltage distributions or of spike rates lasting only several tens of milliseconds, for which slow motion movies are more adequate, obviously precluding online analysis. Finally, the spatial distribution of activity or its properties may be combined with histological data, such as cell type distributions or receptor distributions.

Performing these analyses electrode by electrode on a routine basis is impractical, necessitating automated processing for electrodes within and across experiments. For each scientific question the data will be more or less similar, allowing their processing for specific features in recurring stages. Given the multitude of aspects to analyse and questions to ask, there is, unfortunately, no unique answer as to which tools should be used. Numerous authors have published individual analysis techniques, programmed implementations of tools, or analyzed in detail the pitfalls associated with the interpretation of some of their results or their combinations [133–136]. A description of this work would exceed the scope of this chapter. The collection of such techniques will likely grow as new recording techniques and data acquisition programs appear on the market.

Besides a few commercial software tools (see below), many laboratories have developed their own routines for specific applications and experimental conditions, some of which can be extended as needed but often require some programming knowledge.

Researchers seeking to identify new aspects of network behaviour might be better advised to resort to highly flexible, i.e., programmable analysis tools that allow more control but are less easy to use and sometimes slower in their performance, such as MATLAB (The Mathworks, Natick, Ms., USA), which is widespread in the neuroscience community, NeuroExplorer (Nex Technologies) with its scripting language, or IGOR Pro (WaveMetrics)[5].

[5] Links to data analysis tools:
NeuroExplorer, Nex Technologies, http://www.neuroexplorer.com;
IGOR Pro, WaveMetrics, http://www.wavemetrics.com/Products/IGORPro/IgorPro.html;

The software interfaces of the most widespread data acquisition systems usually allow some online analyses to monitor the experiment and some more complex offline analysis that may require more processing power.

This multitude of complex data acquisition hardware and data analysis tools led to the idea that a platform should be available that allows the applicability and the exchange of analysis tools written for specific acquisition systems and data file formats. For this purpose, a number of hardware developers recently formed the NEUROSHARE forum to design and agree on a common interchange format and public domain standards[6]. The forum also provides a platform for neurophysiology software in general.

9. OUTLOOK

The applications and techniques presented above illustrate the wide range of research questions that can be approached with substrate integrated microelectrode arrays. Beyond the applications mentioned above, substrate integrated arrays have also been used to study acute and cultured brain slices from various brain regions [76,114,137], retinal function and development [98,99], embryonic stem cells [129,138–139] and even whole chicken embryos to study early cardiac development. The option to combine MEAs with conventional electrophysiological techniques, optical measurements, with Ca^{2+}-sensitive dyes and transparent indium-tin Oxide (ITO) electrodes, and additional integrated sensors promises further uses for this technique. The spatio-temporal dynamics of electrical network activity can thus be matched with the spatial distribution and the dynamics of other processes, as well as with anatomical maps of, e.g., receptor distributions gained from immunohistochemical or *in situ* hybridisation studies.

The technical similarity with implantable devices with respect to the materials used and the interface to the tissue facilitates preparatory *in vitro* studies towards neuroprosthetic implants and implantable biosensors [140,141].

Nonetheless, several challenges remain and ask for new developments. On the technical side the viability of the slices should be further improved, in particular for preparations that need to be recorded at physiological temperature or under conditions that elicit high activity. Active cells have a

---

MATLAB, The Mathworks, http://www.mathworks.com/products/matlab;
Plexon Inc., http://www.plexoninc.com.

[6] www.neuroshare.org.

high metabolic demand that needs to be maintained by diffusion alone. Perforated flexible arrays have been proposed and were successfully used for this purpose [142], and will become commercially available in the future. Recent experiments by W. Stein (NMI Reutlingen, personal communication) and in our laboratory indicate that using such arrays with some of the perfusion buffer flowing beneath the slice indeed improves the oxygen availability and the signal–to–noise ratio (SNR) in hippocampal and cerebellar slices. Such arrays should also shorten the time until a drug fully permeates the tissue and thus the response time of the tissue.

Figure 10-15. 8-well multiple MEA recording device. This type of developments is intended either for simultaneous recording from cell cultures or for acute slices (by courtesy of Ayanda Biosystems, Lausanne, CH).

To increase the throughput and cut the costs of experiments using slices in drug research, it is desirable to run several preparations simultaneously. This requires that the systems can run largely unsupervised necessitating highly stable recording, stimulation, perfusion- and drug- application configurations. MEAs potentially enable this approach, in particular with the perspective for new, multi-well plate arrays (Figs. 10-13, 10-15).

To further simplify routine experiments, tissue specific electrode arrangements have been developed that facilitate the reproduction of a tissue-to-electrode configuration while giving the necessary spatial coverage and resolution. One such design is an arrangement that provides a line of electrodes to stimulate the Schaffer Collaterals in the hippocampus and monitor the CA1 region with optimal spatial resolution, e.g., to investigate LTP induction [143]. This trend towards parallelising the recording creates the need for automated, unsupervised data analysis with tools, the results of

which should be robust against variations of SNR, frequency composition and artefacts in the signal. It would further be desirable to reduce the need for single unit analyses that often require extensive pre-processing, e.g., spike sorting, and safeguarding against non-stationarity of the spike generating process.

We expect that the availability of these techniques, of the corresponding data acquisition and data analysis tools, and an increasing number of experimental protocols will contribute to our understanding of signal propagation and information processing in neuronal and cardiac networks, as well as pathological conditions thereof and efforts for their treatment.

10. ACKNOWLEDGEMENTS

The authors would like to thank the German Federal Ministry of Education and Research (BMBF grants 0310964D, 16SV1743 and 01GQ0420), the Land Baden-Württemberg, and the Deutsche Forschungsgemeinschaft (SFB 505) for their support. We would also like to thank C. Boucsein and M. Nawrot for helpful discussions on the manuscript.

11. REFERENCES

[1] Petersen, C.C.H., Sakmann, B., (2000), 'The excitatory neuronal network of rat layer 4 barrel cortex', *J. Neurosci.* **20**, 7539–7546.

[2] Lübke, J., Egger, V., Sakmann, B., Feldmeyer, D., (2000), 'Columnar organization of dendrites and axons of single and synaptically coupled excitatory spiny neurons in layer 4 of the rat barrel cortex', *J. Neurosci.* **20**, 5300–5311.

[3] Chang, F.L.F., Hawrylak, N., Greenough, W.T., (1993), 'Astrocytic and synaptic response to kindling in hippocampal subfield CA1. I. Synaptogenesis in response to kindling *in vitro*', *Brain Res.* **603**, 302–308.

[4] Hawrylak, N., Chang, F.L.F., Greenough, W.T., (1993), 'Astrocytic and synaptic response to kindling in hippocampal subfield CA1. II. synaptogenesis and astrocytic process increases to in vivo kindling', *Brain Res.* **603**, 309–316.

[5] Derouiche, A., Frotscher, M., (1991), 'Astroglial processes around identified glutamatergic synapses contain glutamine synthetase – evidence for transmitter degradation', *Brain Res.* **552**, 346–350.

[6] Yamamoto, M., Honjo, H., Niwa, R., Kodama, I., (1998), 'Low frequency extracellular potentials recorded from the sinoatrial node', *Cardiovasc. Res.* **39**, 360–372.

[7] Spach, M.S., Boineau, J.P., (1997), 'Microfibrosis produces electrical load variations owing to loss of side-to-side cell connections: a major mechanism of structural heart disease arrhythmias', *Pacing & Clinical Electrophysiology* **20**, 397–413.

[8] Spach, M.S., Kootsey, J.M., (1983), 'The nature of electrical propagation in cardiac muscle', *Am. J. Physiol.* **244**, H3–22.

[9] Spach, M.S., (1983), 'The role of cell-to-cell coupling in cardiac conduction disturbances', *Advances in Experimental Medicine & Biology* **161**, 61–77.

[10] Haas, C.A., Frotscher, M., (2004), 'Migration disorders and epilepsy', in: Brain Damage and Repair. From molecular research to clinical therapy, edited by J. M. Delgado-Garcia and T. Herdegen, Kluwer Academic Publishers,.

[11] Haas, C.A., Dudeck, O., Kirsch, M., Huszka, C., Kann, G., Pollak, S., Zentner, J., Frotscher, M., (2002), 'Role for reelin in the development of granule cell dispersion in temporal lobe epilepsy', *J. Neurosci.* **22**, 5797–5802.

[12] Frotscher, M., Haas, C.A., Forster, E., (2003), 'Reelin controls granule cell migration in the dentate gyrus by acting on the radial glial scaffold', *Cereb. Cortex* **13**, 634–640.

[13] Shatz, C.J., (1990), 'Impulse activity and patterning of connections during CNS development', *Neuron* **5**, 745–756.
[14] Goodman, C.S., Shatz, C.J., (1993), 'Developmental mechanisms that generate precise patterns of neuronal connectivity', *Cell* **72**, 77–98.
[15] Shatz, C.J., (1996), 'Emergence of order in visual system development', *Proc. Natl. Acad. Sci. USA*, **93**, 602–608.
[16] Grosshans, D.R., Clayton, D.A., Coultrap, S.J., Browning, M.D., (2002), 'LTP leads to rapid surface expression of NMDA but not AMPA receptors in adult rat CA1', *Nat. Neurosci.* **5**, 27–33.
[17] Beatti, E.C., Stellwagen, D., Morishita, W., Bresnahan, J.C., Ha, B.K., von Zastrow, M., Beattie, M.S., Malenka, R.C., (2002), 'Control of synaptic strength by glial TNFalpha', *Science,* **295**, 2282–2285.
[18] Daw, M. I., Bortolotto, Z.A., Saulle, E., Zaman, S., Collingridge, G.L., Isaac, J.T., (2002), 'Phosphatidylinositol 3 kinase regulates synapse specificity of hippocampal long term depression', *Nat. Neurosci.* **5**, 835–836.
[19] Nitsch, R., Frotscher, M., (1991), 'Maintenance of peripheral dendrites of GABAergic neurons requires specific input', *Brain Res.* **554**, 304–307.
[20] Markram, H., Lübke, J., Frotscher, M., Sakmann, B., (1997), 'Regulation of synaptic efficacy by coincidence of postsynaptic APs and EPSPs', *Science,* **275**, 213–215.
[21] Maletic-Savatic, M., Malinow, R., Svoboda, K., (1999), 'Rapid dendritic morphogenesis in CA1 hippocampal dendrites induced by synaptic activity', *Science,* **283**, 1923–1927.
[22] Lendvai, B., Stern, E.A., Chen, B., Svoboda, K., (2000), 'Experience-dependent plasticity of dendritic spines in the developing rat barrel cortex *in vivo*', *Nature* **404**, 876–881.
[23] Stern, E.A., Maravall, M., Svoboda, K., (2001), 'Rapid development and plasticity of layer 2/3 maps in rat barrel cortex *in vivo*', *Neuron* **31**, 305–315.
[24] Engert, F., Bonhoeffer, T., (1999), 'Dendritic spine changes associated with hippocampal long term synaptic plasticity', *Nature* **399**, 66–70.
[25] Ahissar, E., Vaadia, E., Ahissar, M., Bergman, H., Arieli, A., Abeles, M., (1992), 'Dependence of cortical plasticity on correlated activity of single neurons and on behavioral context', *Science,* **257**, 1412–1415.
[26] Noble, D., (2002), 'Modeling the heart – from genes to cells to the whole organ', *Science,* **295**, 1678–1682.
[27] Feld, Y., Melamed-Frank, M., Kehat, I., Tal, D., Marom, S., Gepstein, L., (2002), 'Electrophysiological modulation of cardiomyocytic tissue by transfected fibroblasts expressing potassium channels: a novel strategy to manipulate excitability', *Circulation* **105**, 522–529.

[28] Rohr, S., Kucera, J.P., Kleber, A.G., (1997), 'Form and function: Impulse propagation in designer cultures of cardiomyocytes', *News in Physiological Sciences* **12**, 171–177.

[29] Spach, M.S., Josephson, M.E., Initiating reentry: The role of nonuniform anisotropy in small circuits', *J. Cardiovasc. Electrophysiol.* **5**, 182–209 (1994).

[30] Spach, M.S., Kootsey, J.M., Sloan, J.D., (1982), 'Active modulation of electrical coupling between cardiac cells of the dog. A mechanism for transient and steady state variations in conduction velocity', *Circ. Res.* **51**, 347–362.

[31] Guevara, M.R., Glass, L., Shrier, A., (1981), 'Phase locking, period-doubling bifurcations, and irregular dynamics in periodically stimulated cardiac cells', *Science*, **214**, 1350–1353.

[32] Wise, K.D., Angell, J. B., Starr, A., (1970), 'An integrated circuit approach to extracellular microelectrodes', *IEEE Trans. Biomed. Eng.* BME-**17**, 238–246.

[33] Bergveld, P., (1972), 'Development, operation and application of the ISFET as a tool for electrophysiology', *IEEE Trans. Biomed. Eng.* **BME-19**, 342–351.

[34] Thomas, C.A., Springer, P.A., Loeb, G.W., Berwald-Netter, Y., Okun, L.M., (1972), 'A miniature microelectrode array to monitor the bioelectric activity of cultured cells', *Exp. Cell Res.* **74**, 61–66.

[35] Bergveld, P., Wiersma, J., Maertens, H., (1976), 'Extracellular potential recording by means of a Field effect transistor without gate metal, called OSFET', *IEEE Trans. Biomed. Eng.* **BME-23**, 136–144.

[36] Gross, G.W., Rieske, E., Kreutzberg, G.W., Meyer, A., (1977), 'A new fixed-array multi-microelectrode system designed for long- term monitoring of extracellular single unit neuronal activity *in vitro*', *Neurosci. Lett.* **6**, 101–105.

[37] Gross, G., (1979), 'Simultaneous single unit recording *in vitro* with a photoetched laser deinsulated gold multimicroelectrode surface', *IEEE Trans. Biomed. Eng.* **BME-26**, 273–279.

[38] Israel, D.A., Barry, W.H., Edell, D.J., Mark, R.G., (1984), 'An array of microelectrodes to stimulate and record from cardiac cells in culture', *Am. J. Physiol.* **247**, H669–H674.

[39] Najafi, K., Wise, K.D., Mochizuki, T., (1985), 'A high-yield IC-compatible multi-channel recording array', *IEEE Transactions on Electron Devices* **ED-32**, 1206–1211.

[40] Gross, G.W., Wen, W., Lin, J.W., (1985), 'Transparent indium–tin oxide electrode patterns for extracellular, multi-site recording in neuronal cultures', *J. Neurosci. Meth.* **15**, 243–252.

[41] Droge, M.H., Gross, G.W., Hightower, M.H., Czisny, L.E., (1986), 'Multielectrode analysis of coordinated, multisite, rythmic bursting in cultured CNS monolayer networks', *J. Neurosci.* **6**, 1583–1592.

[42] Najafi, K. and Wise, K.D., (1986), 'An implantable multielectrode array with on-chip signal processing', *IEEE J. Solid State Circ.* **SC-21**, 1035–1044.

[43] Rohr, S., (1990), 'A computerized device for long term measurements of the contraction frequency of cultured rat heart cells under stable incubating conditions, Pflug. *Arch. Eur. J. Phy.* **416**, 201–206.

[44] Rohr, S., Scholly, D.M., Kleber, A.G., (1991), 'Patterned growth of neonatal rat heart cells in culture morphological and electrophysiological characterization', *Circ. Res.* **68**, 114–130.

[45] Mastrototaro, J.J., Massoud, H.Z., Pilkington, T.C., Ideker, R.E., (1992), 'Rigid and flexible thin-film multielectrode arrays for transmural cardiac recording', *IEEE Trans. Biomed. Eng.* **39**, 271–379.

[46] Eckhorn, R. and Thomas, U., (1993), 'A new method for the insertion of multiple microprobes into neural and muscular tissue, including fiber electrodes, fine wires, needles and microsensors', *J. Neurosci. Meth.* **49**, 175–179.

[47] Hoogerwerf, A.C. and Wise, K.D., (1994), 'A three-dimensional microelectrode array for chronic neural recording', *IEEE Trans. Biomed. Eng.* **41**, 1136–1146.

[48] Nádasny, Z., Csicsvari, J., Penttonen, M., Hetke, J., Wise, K., Buzsáki, G., (1998), 'Extracellular recording and analysis of neuronal activity: from single cells to ensembles, in: Neuronal Ensembles: Startegies for recording and decoding', edited by H. B. Eichenbaum and J. L. Davis, (Wiley-Liss, New York, , 17–55.

[49] Mohr, G., Hofer, E., Plank, G., (1999), 'A new real-time mapping system to detect microscopic cardiac excitation patterns', *Biomed. Instrum. Technol.* **33**, 455–461.

[50] Sprössler, C., Denyer, M., Britland, S., Knoll, W., Offenhäusser, A., (1999), 'Electrical recordings from rat cardiac muscle cells using field-effect transistors', *Phys. Rev.* **E 60**, 2171–2176.

[51] Bai, Q. and Wise, K.D., (2001), 'Single-unit neural recording with active microelectrode arrays', *IEEE Trans. Biomed. Eng.* **48**, 911–920.

[52] Nicolelis, M.A., Dimitrov, D., Carmena, J.M., Crist, R., Lehew, G., Kralik, J.D., Wise, S.P., (2003), 'Chronic, multisite, multielectrode recordings in macaque monkeys', *Proc. Natl. Acad. Sci. USA,* **100**, 11041–11046.

[53] Tominaga, T., Tominaga, Y., Ichikawa, M., (2001), 'Simultaneous multi-site recordings of neural activity with an inline multielectrode

array and optical measurement in rat hippocampal slices', *Pflug. Arch. Eur. J. Phy.* **443**, 317–322.

[54] Cohen, D., Yarom, Y., (1999), 'Optical measurements of synchronized activity in isolated mammalian cerebellum', *Neuroscience* **94**, 859–866.

[55] Ebner, T. J., Chen, G., (1995), 'Use of voltage-sensitive dyes and optical recordings in the central nervous system', *Prog. Neurobiol.* **46**, 463–506.

[56] Rohr, S. and Salzberg, B.M., (1994), 'Multiple site optical recording of transmembrane voltage (MSORTV) in patterned growth heart cell cultures: Assessing electrical behavior, with microsecond resolution, on a cellular and subcellular scale', *Biophys. J.* **67**, 1301–1315.

[57] Grinvald, A., Frostig, R.D., Siegel, R.M., Bartfeld, E., (1991), 'High-Resolution Optical Imaging of Functional Brain Architecture in the Awake Monkey', *Proc. Natl. Acad. Sci. USA,* **88**, 11559–11563.

[58] Grinvald, A., (1985), 'Real time optical mapping of neuronal activity: From single growth cones to intact mammalian brain', *Ann. Rev. Neurosci.* 8, **263**.

[59] Windisch, H., Mueller, W., Tritthart, H.A., (1985), 'Fluorescence monitoring of rapid changes in membrane potential in heart muscle', *Biophys. J.* **48**, 877–884.

[60] Vassanelli, S. , Fromherz, P., (1997), 'Neurons from rat brain coupled to transistors', *App. Phys. A–Solids & Surfaces* **65**, 85–88.

[61] Fromherz, P., Offenhäusser, A., Vetter, T., Weis, J., (1991), 'A neuron-silicon junction: a Retzius cell of the leech on an insulated-gate field-effect transistor', *Science,* **252**, 1290.

[62] Fromherz, P., (2003), 'Neuroelectronic interfacing: semiconductor chips with ion channels, nerve cells and brain', in: Nano-electronics and Information Technology, Waser, R., (ed.), Wiley-VCH, Berlin, 781–810.

[63] Zeck, G., Fromherz, P., (2001), 'Noninvasive neuroelectronic interfacing with synaptically connected snail neurons immobilized on a semiconductor chip', *Proc. Natl. Acad. Sci. USA,* **98**, 10457–10462.

[64] Hetke, J.F.,erson, D.J., (2004), 'Silicon electrodes for extracellular recording, in: Handbook of neuroprosthetic methods', Peterson, J.K., Finn, W.E., Lopresti, P.G., (eds.), CRC Press, Boca Raton, 163–191.

[65] Schwartz, A.B., (2004), 'Cortical neural prosthetics', *Ann. Rev. Neurosci.* **27**, 487–507.

[66] Rutten, W. L., Smit, J.P., Frieswijk, T.A., Bielen, J.A., Brouwer, A.L., Buitenweg, J.R., Heida, C., (1999), 'Neuro-electronic interfacing with multielectrode arrays', *IEEE Eng. Med. Biol. Mag.* **18**, 47–55.

[67] Bi, G.Q. , Poo, M.M., (1998), 'Synaptic modifications in cultured hippocampal neurons: dependence on spike timing, synaptic strength, and postsynaptic cell type', *J. Neurosci.* **18**, 10464–10472.

[68] Eytan, D., Brenner, N., Marom, S., (2003), 'Selective adaptation in networks of cortical neurons', *J. Neurosci.* **23**, 9349–9356.

[69] Marom, S. and Shahaf, G., (2002), 'Development, learning and memory in large random networks of cortical neurons: lessons beyond anatomy', *Q. Rev. Biophys.* **35**, 63–87.

[70] Shahaf, G. and Marom, S., (2001), 'Learning in networks of cortical neurons', *J. Neurosci.* **21**, 8782–8788.

[71] Tal, D., Jacobson, E., Lyakhov, V., Marom, S., (2001), 'Frequency tuning of input-output relation in a rat cortical neuron *in vitro*', *Neurosci. Lett.* **300**, 21–24.

[72] Jimbo, Y. and Robinson, H.P., (2000), 'Propagation of spontaneous synchronized activity in cortical slice cultures recorded by planar electrode arrays', *Bioelectrochemistry* **51**, 107–115.

[73] Jimbo, Y., Kawana, A., Parodi, P., Torre, V., (2000), 'The dynamics of a neuronal culture of dissociated cortical neurons of neonatal rats', *Biol. Cybern.* **83**, 1–20.

[74] van Ooyen, A., (ed.), (2003), 'Modeling Neural Development', The MIT Press, Cambridge MA, London,.

[75] Streit, J., Tscherter, A., Heuschkel, M.O., Renaud, P., (2001), 'The generation of rhythmic activity in dissociated cultures of rat spinal cord', *Eur. J. Neurosci.* **14**, 191–202.

[76] Tscherter, A., Heuschkel, M.O., Renaud, P., Streit, J., (2001), 'Spatiotemporal characterization of rhythmic activity in rat spinal cord slice cultures', *Eur. J. Neurosci.* **14**, 179–190.

[77] Gross, G.W., Harsch, A., Rhoades, B.K., Göpel, W., (1997), 'Odor, drug and toxin analysis with neuronal networks *in vitro*: extracellular array recording of network responses', *Biosens. Bioelectron.* **12**, 373–393.

[78] Gross, G.W., Rhoades, B.K., Azzazy, H.M., Wu, M.C., (1995), 'The use of neuronal networks on multielectrode arrays as biosensors', *Biosens. Bioelectron.* **10**, 553–567.

[79] Gramowski, A., Schiffmann, D., Gross, G.W., (2000), 'Quantification of acute neurotoxic effects of trimethyltin using neuronal networks cultured on microelectrode arrays', *Neurotoxicology*, **21**, 331–342.

[80] Lipton, P., Aitken, P.G., Dudek, F.E., Eskessen, K., Espanol, M.T., Ferchmin, P.A., Kelly, J.B., Kreisman, N.R., Landfield, P.W., Larkman, P.M., (1995), 'Making the best of brain slices: comparing preparative methods', *J. Neurosci. Meth.* **59**, 151–156.

[81] Alger, B.E., Dhanjal, S.S., Dingledine, R., Garthwaite, J., Henderson, G., King, G.L., Lipton, P., North, A., Schwartzkroin, P.A., Sears, T.A., Segal, M., Whittingham, T.S., Williams, J., (1984), 'Brain Slice Methods', in: Brain Slices, Dingledine, R., (ed.), Plenum Press, New York, 406.

[82] Gaehwiler, B.H., (1988), 'Organotypic cultures of neural tissue', *Trends Neurosci.* **11**, 484–489.

[83] Robert, F., Corrèges, P., Duport, S., Stoppini, L., (2001), 'Combined electrophysiology and microdialysis on hippocampal slice cultures using the physiocard®system', *Current Separations* **16**, 3–10.

[84] Stoppini, L., Duport, S., Corrèges, P., (1997), 'A new extracellular multi-recording system for electrophysiological studies: application to hippocampal organotypic cultures. *J. Neurosci. Meth.* **72**, 23–33.

[85] Thiébaud, P., de Rooij, N.F., Koudelka-Hep, M., Stoppini, L., (1997), 'Microelectrode arrays for electrophysiological monitoring of hippocampal organotypic slice cultures', *IEEE Trans. Biomed. Eng.* **44**, 1159–1163.

[86] Stoppini, L., Buchs, P.A., Muller, D., (1991), 'A simple method for organotypic cultures of nervous tissue', *J. Neurosci. Meth.* **37**, 173–182.

[87] Egert, U., Schlosshauer, B., Fennrich, S., Nisch, W., Fejtl, M., Knott, Th., Müller, T., Hämmerle, H., (1998), 'A novel organotypic long term culture of the rat hippocampus on substrate-integrated multielectrode arrays', *Brain Res. Prot.* **2**, 229–242.

[88] Knott, Th., (2001), 'Population synchronization during propagation of epileptiform activity in organotypic hippocampal slices—a microelectrode array study', Der Andere Verlag, Osnabrueck.

[89] Malmivuo, J., Plonsey, R., (1995), 'Bioelectromagnetism: Principles and applications of bioelectric and biomagnetic fields', Oxford University Press, USA.

[90] Heuschkel, M.O., Fejtl, M., Raggenbass, M., Bertrand, D., Renaud, P., (2002), 'A three-dimensional multi-electrode array for multi-site stimulation and recording in acute brain slices', *J. Neurosci. Meth.* **114**, 135–148.

[91] Heuschkel, M.O., (2001), 'Fabrication of multielectrode array devices for electrophysiological monitoring of *in vitro* cell/tissue cultures', in Series in Microsystems, Besse, P.A., Gijs, M., Popvic, R.S., Renaud, P., Hartung-Gorre Verlag, Konstanz.

[92] Janders, M., Egert, U., Stelzle, M., Nisch, W., (1996), 'Novel thin-film titanium nitride micro-electrodes with excellent charge transfer capability for cell stimulation and sensing applications', *Bridging Disciplines for Biomedicine, Proceedings of the 18th Annual*

Conference of the IEEE Engineering in Medicine and Biology Society, 48–49

[93] Rosenberg, L.J., Jordan, R.S., Gross, G.W., Emery, D.G., Lucas, J.H., (1996), 'Effects of methylprednisolone on lesioned and uninjured mammalian spinal neurons: viability, ultrastructure, and network electrophysiology', *J. Neurotrauma* **13**, 417–437.

[94] Jimbo, Y., Tateno, T., Robinson, H.P., (1999), 'Simultaneous induction of pathway-specific potentiation and depression in networks of cortical neurons', *Biophys. J.* **76**, 670–678.

[95] Kamioka, H., Maeda, E., Jimbo, Y., Robinson, H.P.C., Kawana, A., (1996), 'Spontaneous periodic synchronized bursting during formation of patterns of connections in cortical cultures', *Neurosci. Lett.* **206**, 109–112.

[96] Potter, S.M., (2001), 'Distributed processing in cultured neuronal networks', Prog. *Brain Res.* **130**, 49–62.

[97] Potter, S.M. and DeMarse, T.B., (2001), 'A new approach to neural cell culture for long term studies', *J. Neurosci. Meth.* **110**, 17–24.

[98] Wong, R.O.L., Meister, M., Shatz, C.J., (1993), 'Transient period of correlated bursting activity during development of the mammalian retina', *Neuron* **11**, 923–938.

[99] Meister, M., Wong, R.O.L., Baylor, D.A., Shatz, C.J., (1991), 'Synchronous bursts of action potentials in ganglion cells of the developing mammalian retina', *Science*, **252**, 939–943.

[100] Egert, U., Heck, D., Aertsen, A., (2002), '2-Dimensional monitoring of spiking networks in acute brain slices', *Exp. Brain Res.* **142**, 268–274.

[101] Grattarola, M. , Martinoia, S., (1993), 'Modeling the neuron-microtransducer junction—from extracellular to patch recording', *IEEE Trans. Biomed. Eng.* **40**, 35–41.

[102] Rall, W., (1969), 'Distribution of potential in cylindrical coordinates and time constants for a membrane cylinder', *Biophys. J.* **9**, 1509–1541.

[103] Plonsey, R., (1977), 'Action potential sources and their volume conductor fields', *Proc. IEEE* **65**, 601–611.

[104] Henze, D.A., Borhegyi, Z., Csicsvari, J., Mamiya, A., Harris, K.D., Buzsáki, G., (2000), 'Intracellular features predicted by extracellular recordings in the hippocampus *in vivo*', *J. Neurophysiol.* **84**, 390–400.

[105] Halbach, M.D., Egert, U., Hescheler, J., Banach, K., (2003), 'Estimation of action potential changes from field potential recordings in multi-cellular mouse cardiac myocyte cultures', *Cell. Physiol. Biochem*. **13**, 271–284.

[106] Shimono, K., Brucher, F., Granger, R., Lynch, G., Taketani, M., (2000), 'Origins and distribution of cholinergically induced beta rhythms in hippocampal slices', *J. Neurosci.* **20**, 8462–8473.
[107] Mitzdorf, U., Singer, W., (1977), 'Laminar segregation of afferents to lateral geniculate nucleus of the cat: an analysis of current source density', *J. Neurophysiol.* **40**, 1227–1244.
[108] Novak, J.L. and Wheeler, B.C., (1989), 'Two-dimensional current source density analysis of propagation delays for components of epileptiform bursts in rat hippocampal slices', *Brain Res.* **497**, 223–230.
[109] Wheeler, B.C. and Novak, J.L., (1986), 'Current source density estimation using microelectrode array data from the hippocampal slice preparation', *IEEE Trans. Biomed. Eng.* **BME-33**, 1204–1213.
[110] Freeman, J.A. and Nicholson, C., (1975), 'Experimental optimization of current source-density technique for anuran cerebellum', *J. Neurophysiol.* **38**, 369–382.
[111] Nicholson, C. and Llinas, R., (1975), 'Real time current source-density analysis using multi-electrode array in cat cerebellum', *Brain Res.* **100**, 418–424.
[112] Haberly, L.B. and Shepherd, G.M., (1973), 'Current density analysis of summed evoked potentials in opossum prepyriform cortex', *J. Physiol. (Lond.)* **36**, 789–803.
[113] Nicholson, C. and Llinas, R., (1971), 'Field potentials in the alligator cerebellum and theory of their relationship to Purkinje cell dendritic spikes', *J. Neurophysiol.* **34**, 509–531.
[114] Stett, A., Egert, U., Guenther, E., Hofmann, F., Meyer, Th., Nisch, W., Hämmerle, H., (2003), 'Biological applications of micro-electrode arrays in drug discovery and basic research', *Analytical and Bioanalytical Chemistry* **377**, 486–495.
[115] Tian, N. and Copenhagen, D.R., (2001), 'Visual deprivation alters development of synaptic function in inner retina after eye opening', *Neuron* **32**, 439–449.
[116] Tian, N. and Copenhagen, D.R., (2003), 'Visual stimulation is required for refinement of ON and OFF pathways in postnatal retina', *Neuron* **39**, 85–96.
[117] Streit, J., (1993), 'Regular oscillations of synaptic activity in spinal networks invitro', *J. Neurophysiol.* **70**, 871–878.
[118] Tousson E., Meissl, H., (2004), 'Supra-chiasmatic nuclei grafts restore the circadian rhythm in the paraventricular nucleus of the hypothalamus', *J. Neurosci.* **24**, 2983–2988.
[119] Egert, U. and Hämmerle, H., (2002), 'Application of the microelectrode-array (MEA) technology in pharmaceutical drug

research, in: Sensoren im Fokus neuer Anwendungen', edited by Baselt, J.P., Gerlach, G., w.e.b. Universitätsverlag, Dresden, 51–54.

[120] Knott, Th., Fejtl, M., Schlosshauer, B., Egert, U., Aertsen, A., Hämmerle, H., (1999), 'Long term monitoring of *in vitro* epileptogenesis: study of e/s-potentiation in organotypic hippocampal slices using a micro-electrode-array', *Soc. Neurosci. Abstr.* **25**, 217.5.

[121] Knott, Th., Egert, U., Hehl, U., Hämmerle, H., Aertsen, A., (2000), 'Synchronization in propagating epileptiform population spikes in organotypic hippocampal slices—experiments and models', *22. Reutlingen. International meeting on substrate-integrated microelectrode arrays: hard-, soft-, and wetware*.

[122] Gray, C.M., König, P., Engel, A.K., Singer, W., (1989), 'Oscillatory responses in cat visual cortex exhibit inter-columnar synchronization which reflects global stimulus properties', *Nature* **338**, 334–337.

[123] Bouthenet, M.L., Souil, E., Martres, M.P., Sokoloff, P., Giros, B., Schwartz, J.C., (1991), 'Localization of dopamine D3 receptor mRNA in the rat brain using in situ hybridization histochemistry: comparison with dopamine D2 receptor mRNA', *Brain Res.* **564**, 203–219.

[124] Jost, B., Aertsen, A., Egert, U., (2002), 'Dopamine D2/D3 receptor mediated modulation of cerebellar spike activity', *FENS Abstr.* **1**, A012.11.

[125] Jost, B., (2001), 'Dopamine receptor mediated modulation of cerebellar spike activity', Diploma, Universität Freiburg.

[126] Redfern, W.S., Carlsson, L., Davis, A.S., Lynch, W., MacKenzie, G.I., Palethorpe, S., Siegl, P.K., Strang, I., Sullivan, A. T., Wallis, R., Camm, A.J., Hammond, T.G., (2003), 'Relationships between preclinical cardiac electrophysiology, clinical QT interval prolongation and torsade de pointes for a broad range of drugs: evidence for a provisional safety margin in drug development', *Cardiovasc. Res.* **58**, 32–45.

[127] Fermini, B., Fossa, A.A., (2003), 'The impact of drug-induced QT interval prolongation on drug discovery and development', *Nat. Rev. Drug Discov.* **2**, 439–447.

[128] Vieweg, W.V.R., (2002), 'Mechanisms and risks of electrocardiographic QT interval prolongation when using antipsychotic drugs', *J. Clin. Psychiatry* **63**, 18–24.

[129] Igelmund, P., Fleischmann, B.K., Fischer, I.V., Soest, J., Gryshchenko, O., Sauer, H., Liu, Q., Hescheler, J., (1999), 'Action potential propagation failures in long term recordings from embryonic stem cell-derived cardiomyocytes in tissue-culture', *Pflug. Arch. Eur. J. Phy.* **437**, 669–679.

[130] Rohr, S., Kucera, J.P., Fast, V.G., Kleber, A.G., (1997), 'Paradoxical improvement of impulse conduction in cardiac tissue by partial cellular uncoupling', *Science*, **275**, 841–844.
[131] Lazarra, R., (1993), 'Antiarrhythmic drugs and torsade de pointes', *Eur. Heart J.* **44**, 88–92.
[132] Meyer, T., Boven, K.-H., Guenther, E., Fejtl, M., (2004), 'Micro-Electrode Arrays (MEA) – a novel tool in cardiac safety pharmacology to study QT-prolongation', *Drug Safety* **27**. 763-772
[133] Bar-Gad, I., Ritov, Y., Vaadia, E., Bergman, H., (2001), 'Failure in identification of overlapping spikes from multiple neuron activity causes artificial correlations', *J. Neurosci. Meth.* **107**, 1–13.
[134] Wheeler, B.C. and Heetderks, W.J., (1982), 'A comparison of techniques for classification of multiple neural signals', *IEEE Trans. Biomed. Eng.* **29**, 752–759.
[135] Ben Shaul, Y., Bergman, H., Ritov, Y., Abeles, M., (2001), 'Trial to trial variability in either stimulus or action causes apparent correlation and synchrony in neuronal activity', *J. Neurosci. Meth.* **111**, 99–110.
[136] Abeles, M., (1982), 'Quantification, smoothing, and confidence limits for single-unitshistograms', *J. Neurosci. Meth.* **5**, 317–325.
[137] Beggs, J.M. and Plenz, D., (2004), 'Neuronal avalanches in neocortical circuits', *J. Neurosci.* **23**, 11167–11177.
[138] Banach, K., Halbach, M., Hu, P., Hescheler, J., Egert, U., (2003), 'Development of electrical activity in cardiac myocyte aggregates derived from mouse embryonic stem cells', *Am. J. Physiol.* **284**, H2114–H2123.
[139] Kehat, I., Gepstein, A., Spira, A., Itskovitz-Eldor, J., Gepstein, L., (2002), 'High-resolution electrophysiological assessment of human embryonic stem cell-derived cardiomyocytes: a novel *in vitro* model for the study of conduction', *Circ. Res.* **91**, 659–661.
[140] Stett, A., Barth, W., Weiss, S., Hämmerle, H., Zrenner, E., (2000), 'Electrical multi-site stimulation of the isolated chicken retina', *Vision Res.* **40**, 1785–1795.
[141] Zrenner, E., Stett, A., Weiss, S., Aramant, R.B., Guenther, E., Kohler, K., Miliczek, K.D., Seiler, M.J., Hämmerle, H., (1999), 'Can subretinal microphotodiodes successfully replace degenerated photoreceptors?', *Vision Res.* **39**, 2555–2567.
[142] Boppart, S.A., Wheeler, B.C., Wallace, C.S., (1992), 'A flexible perforated microelectrode array for extended neural recordings', *IEEE Trans. Biomed. Eng.* **39**, 37–42.
[143] Gholmieh, G., Soussou, W., Courellis, S., Marmarelis, V., Berger, T., Baudry, M., (2001), 'A biosensor for detecting changes in cognitive

processing based on nonlinear systems analysis', *Biosens. Bioelectron.* **16**, 491–501.